UNITED NATIONS EDUCATIONAL, SCIENTIFIC AND CULTURAL ORGANIZATION
INTERNATIONAL ATOMIC ENERGY AGENCY
INTERNATIONAL CENTRE FOR THEORETICAL PHYSICS
I.C.T.P., P.O. BOX 586, 34100 TRIESTE, ITALY, CABLE: CENTRATOM TRIESTE

SMR/1006 - 26

COURSE ON "OCEAN-ATMOSPHERE INTERACTIONS IN THE TROPICS"
26 May - 6 June 1997

"The Atmospheric Response to Tropical Heat Anomalies"

D. BATTISTI
Dept of Atmospheric Sciences
University of Washington
Seattle WA
USA

Please note: These are preliminary notes intended for internal distribution only.

THE ATMOSPHERIC RESPONSE TO TROPICAL HEAT ANOMALIES

1) DRIVING OF THE TROPICAL ATMOSPHERE

- Diabatic Heating:
  - Latent Heat Release Q_o
  - Virtual Sensible Heat Flux Q_{VS} (vapor + temperature induced buoyancy changes)

- Latent Heat Release in convective Clouds

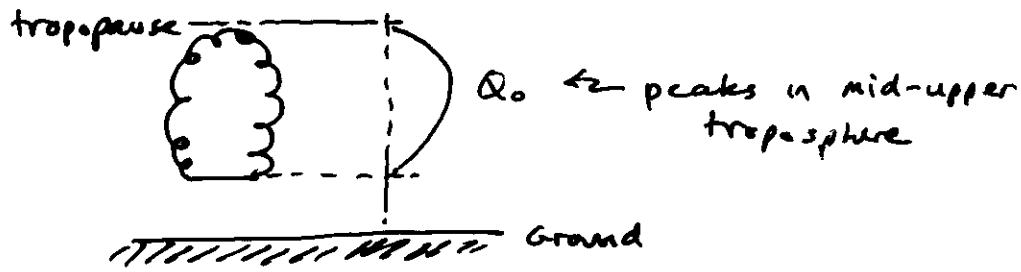

- Sensible Heat Flux and evaporation changes Q_{VS} at the surface ⇒

  changes in Temperature and vapor mass in boundary layer ⇒

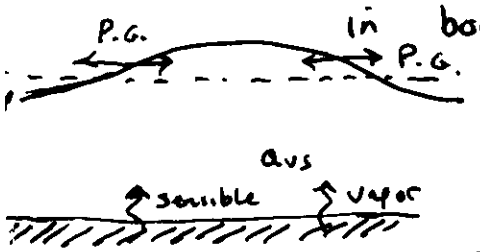

  density change in planetary boundary layer (PBL) ⇒

  changes in pressure gradients (P.G.) ⇒ circulation anomalies in PBL

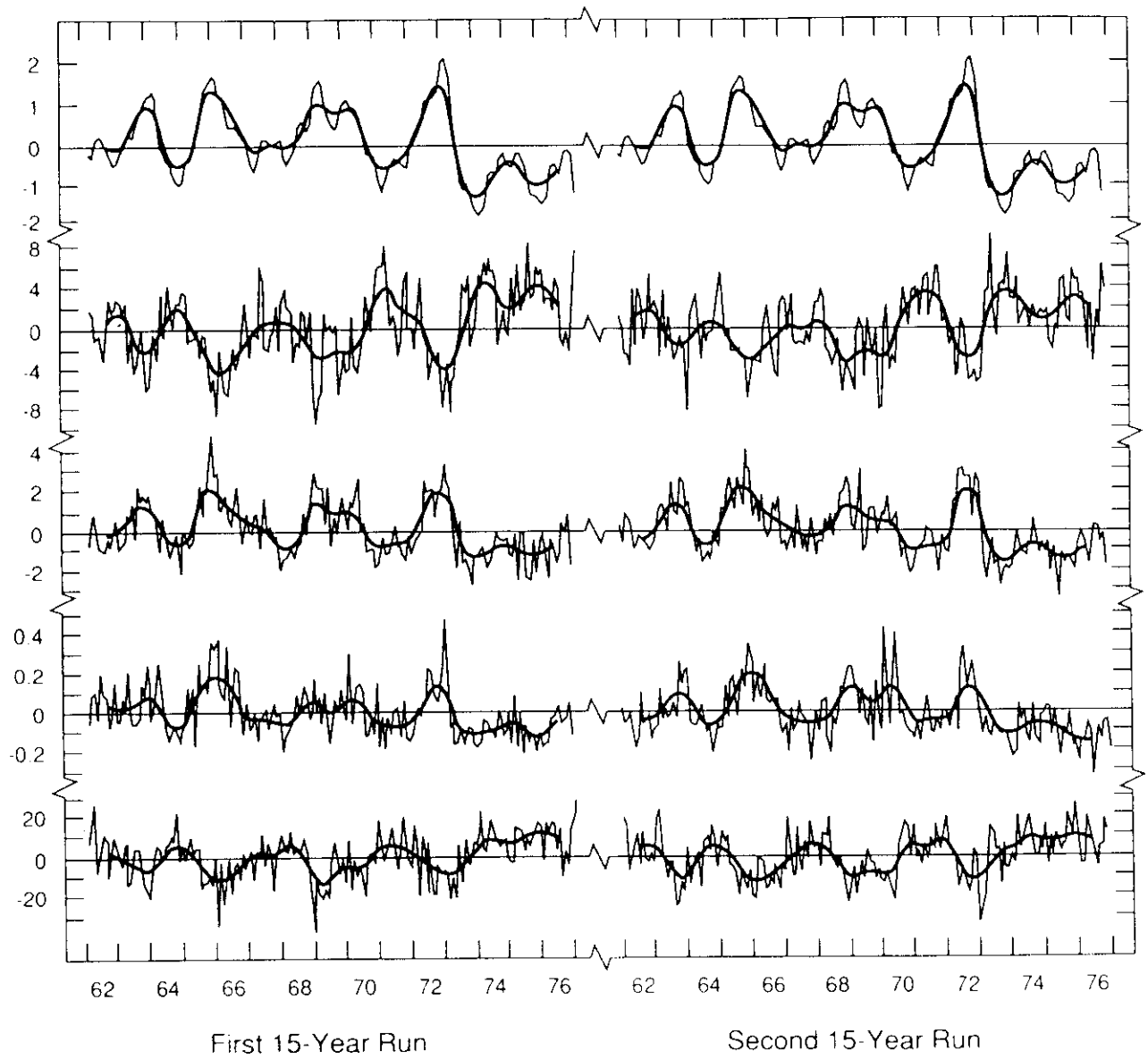

Fig. 19.7 Time series of monthly (light curves) and lowpass filtered (heavy curves) anomalies of sea surface temperature, zonal wind at 200 and 950 mb, precipitation rate, and difference in 1,000 mb height between Tahiti and Darwin, for two independent 15-year model simulations. The tropical indices are computed using data for the central equatorial Pacific. From Lau (1985).

2) THE DEEP TROPICAL RESPONSE TO CONVECTIVE INDUCED HEATING ANOMALIES

a) The Vertical Structure of the excited Waves

Heating generates spectrum of waves (kelvin, Rossby, Gravity, etc.) that propagate horizontally and vertically

Fig

As the frequency (ω) of the forcing → zero, the vertical energy propagation → zero, too.

∴ Low frequency (period ≳ 20 days) energy is strongly trapped to the levels of the heating.

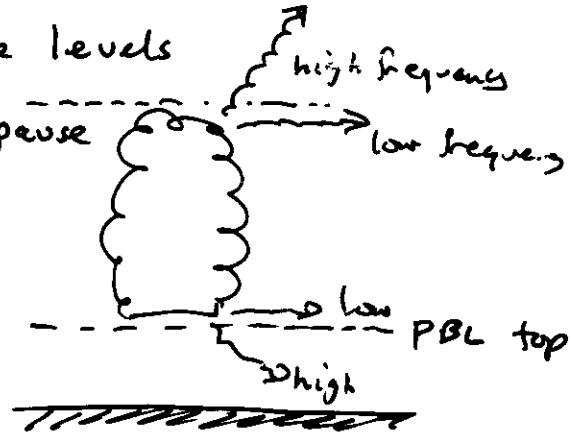

Hence, the tropopause (top of convection) is effectively a lid to the low frequency waves which propagate ~ horizontally.

One can prove (see notes), in the tropics diabatic heating (J) must be balanced closely by adiabatic motion (w)...

Otherwise quasigeostrophic flow would be dynamically unstable:

(i) $\left| \underset{\sim}{k} \times \frac{\partial \underset{\sim}{u}_g}{\partial z} \right| \propto \left| \underset{\sim}{\nabla} T / f \right|$

as $y \to 0$, $f \to 0$ and thus $\left| \frac{\partial \underset{\sim}{u}_g}{\partial z} \right| \to \infty$ unless $\left| \underset{\sim}{\nabla} T \right| \to 0$

↑ unstable baroclinically

(ii) Since

$$\frac{D}{Dt} T = \frac{\partial T}{\partial t} + \underset{\sim}{u} \cdot \nabla T + w \left(\frac{N^2 H}{R} \right) = J / c_p$$

at low frequencies

$$\frac{DT}{Dt} \simeq w \left(\frac{N^2 H}{R} \right) = J / c_p \qquad (3.1)$$

Together, we find...

In the low frequency limit, the vertical structure is essentially the gravest baroclinic mode of the free troposphere:

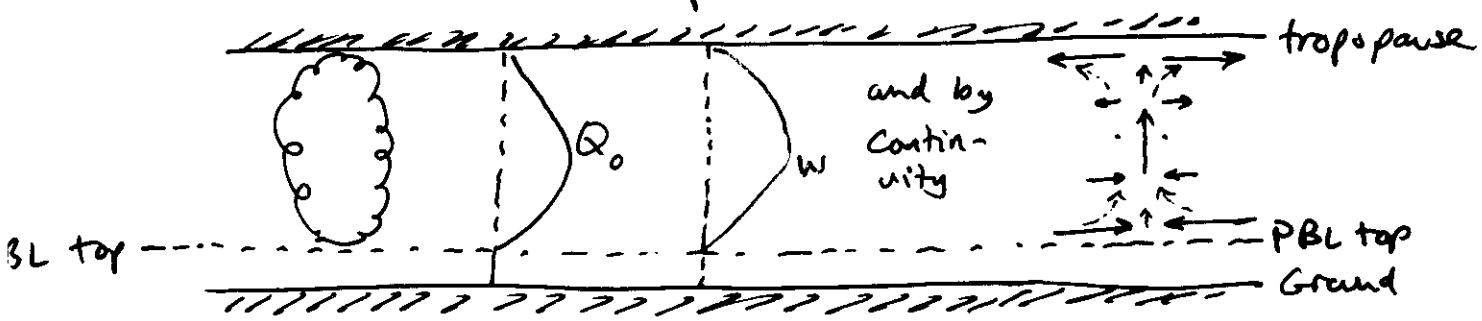

b) The Horizontal Solutions

reduce to the linear shallow water model on an equatorial β-plane (lect. 2A):

$$\frac{\partial \underline{u}}{\partial t} - \underline{\underline{k}}\,\beta y \times \underline{u} = -\nabla \phi \qquad (3.2)$$

$$\frac{\partial \phi}{\partial t} + c_0^2 \nabla \cdot \underline{u} = -J/c_p = -Q_0 \qquad (3.3)$$

where $c_0 = NH$ is the speed of the gravest baroclinic mode. [note: eqn.(3.3) is from continuity, ideal gas and thermodynamic eqn ($w \propto Q$)]

$\Rightarrow$ Matsuno's (1966) Dispersion Relationship describes the modal solutions. At low frequency Figs the key modes are Kelvin and Rossby set (long)

(i) Kelvin

$$u = \phi/c_0 = G(x - c_0 t)\exp\left(-\frac{y^2\beta}{2c_0}\right) \qquad (3.4)$$

$v = 0$; eastward at speed c_0

(ii) Rossby Waves (long)

u, ϕ, v complicated $\qquad c_n = \frac{c_0}{2n+1}$; $n = 1, 2, \ldots$ (3.5)

Figs

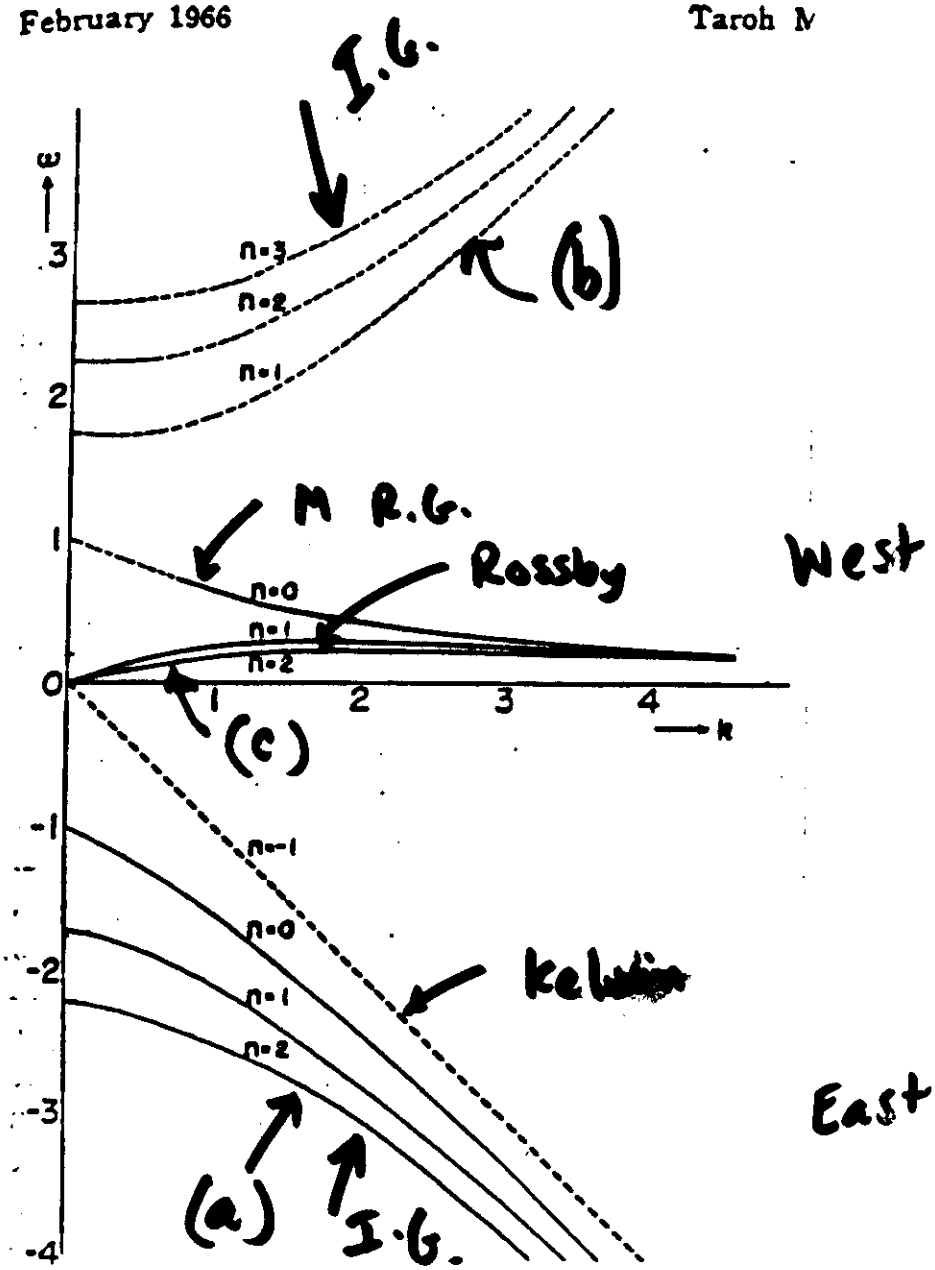

Fig. 3a. Frequencies as functions of wave number.
Thin solid line: eastward propating inertio-gravity waves.
Thin dashed line: westward propagating inertio-gravity waves.
Thick solid line: Rossby (quasi-geostrophic) waves.
Thick dashed line: The Kelvine wave like wave.

n=1 n=2

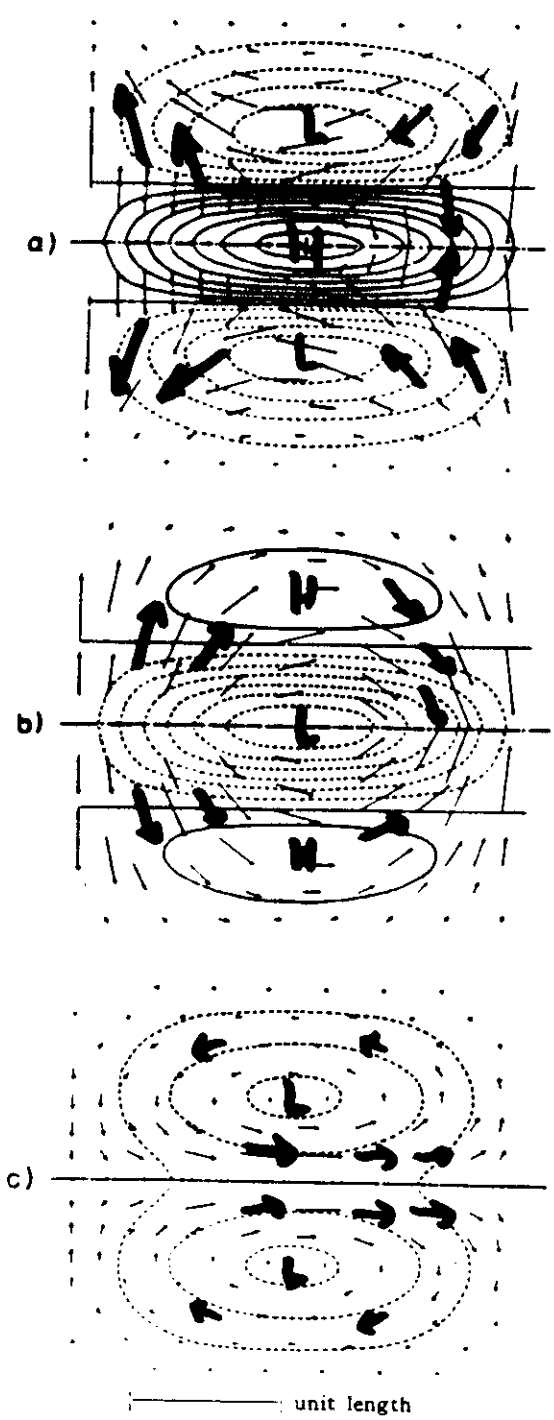

Fig. 4. Pressure and velocity distributions of eigensolutions for $n=1$
a: Eastward propagating inertio-gravity wave
b: Westward propagating inertio-gravity wave
c: Rossby wave.

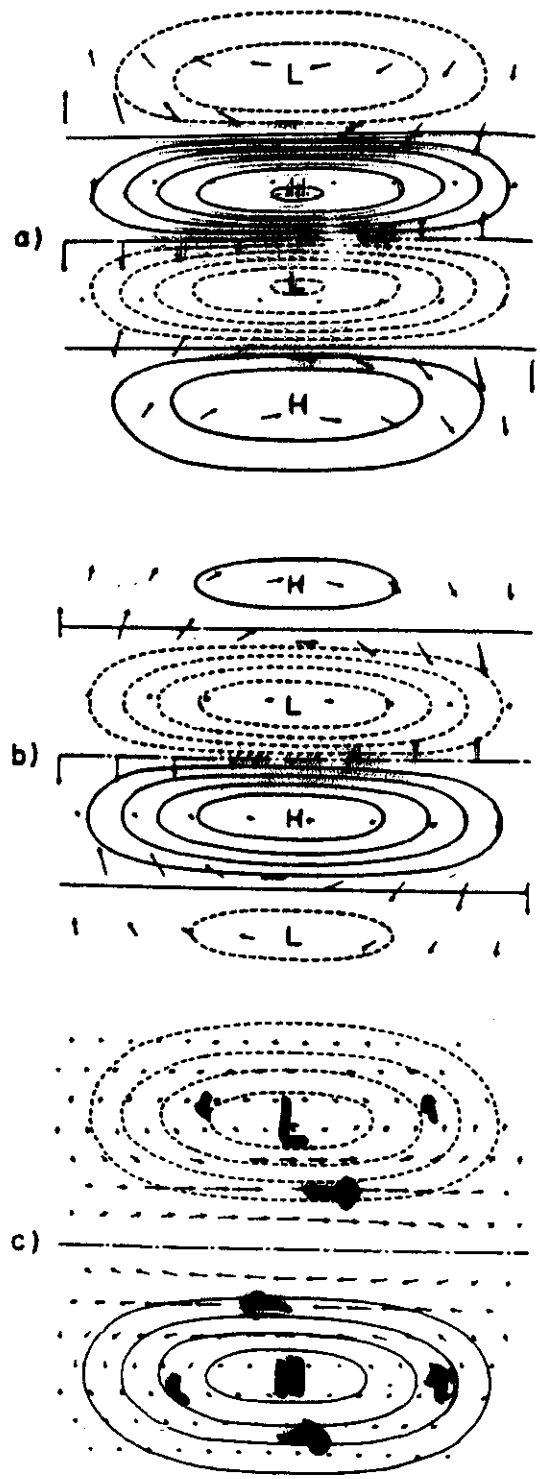

Fig. 5. Same as Fig. 4 but for $n=2$.

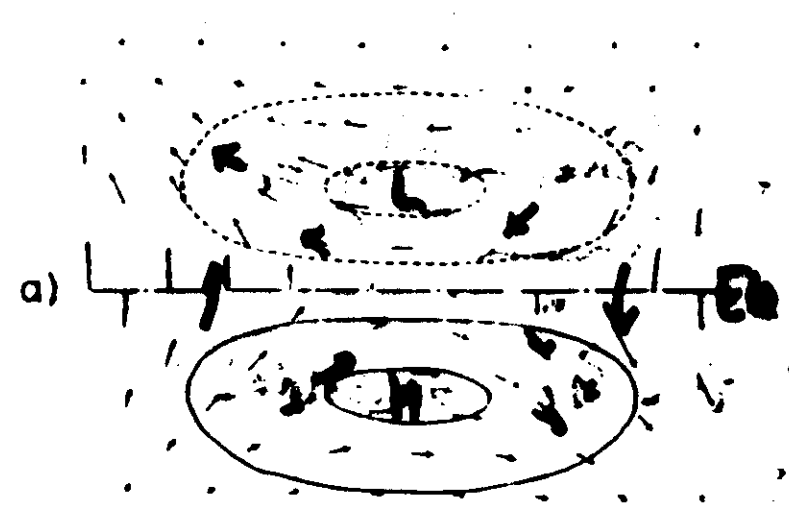

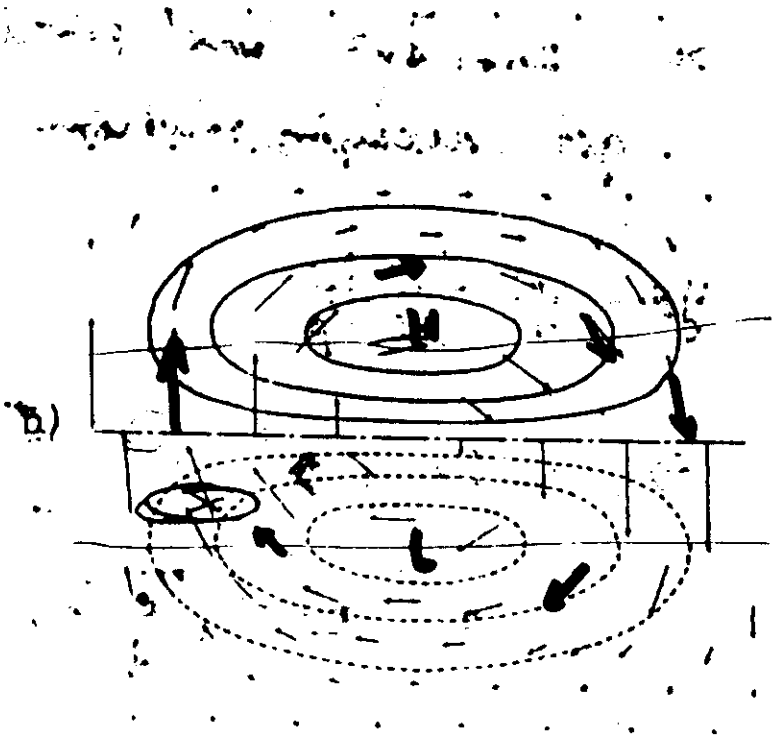

Fig. 6. Pressure and velocity distributions of eigensolutions for $n=0$ and $k=0.5$
a: Eastward moving inertio-gravity wave
b: Westward moving inertio-gravity wave.

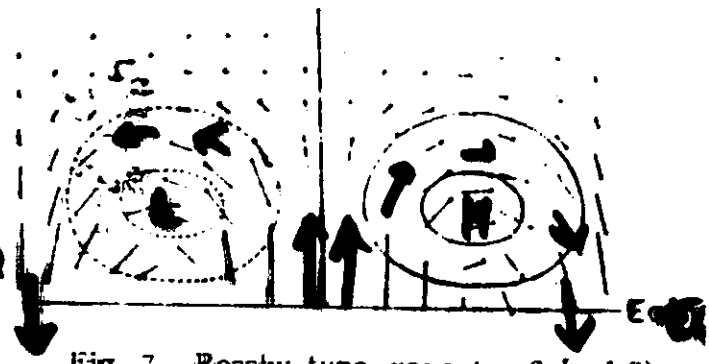

Fig. 7. Rossby type wave ($n=0$ $k=1.0$).

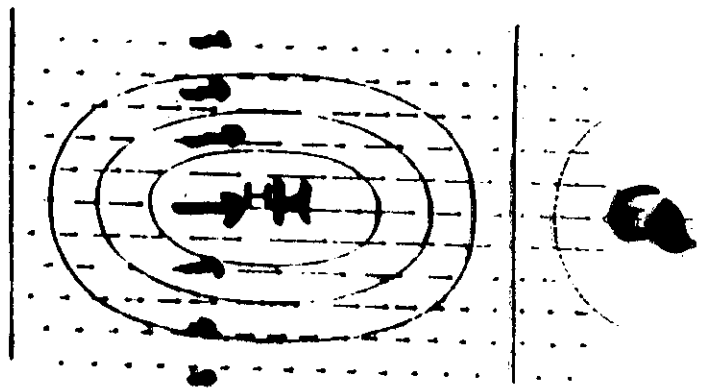

Fig. 8. Pressure and velocity distributions of eigensolution for $n=-1$ and $k=0.5$.
This wave behaves like as the Kelvin wav

Typical Scales

	C_0 (m/s)	Kelvin scale Meridional E-folding
ocean	2.5	470 km
atmosphere (troposphere)	60	2200 km

The Gill Model (Gill, 1980)

An equilibrium (steady) model of the linear, gravest vertical mode response of the tropical atmosphere to prescribed convective heating anomaly Q_0. Gill's model is the steady form of eqns (3.2), (3.3). (with damping).

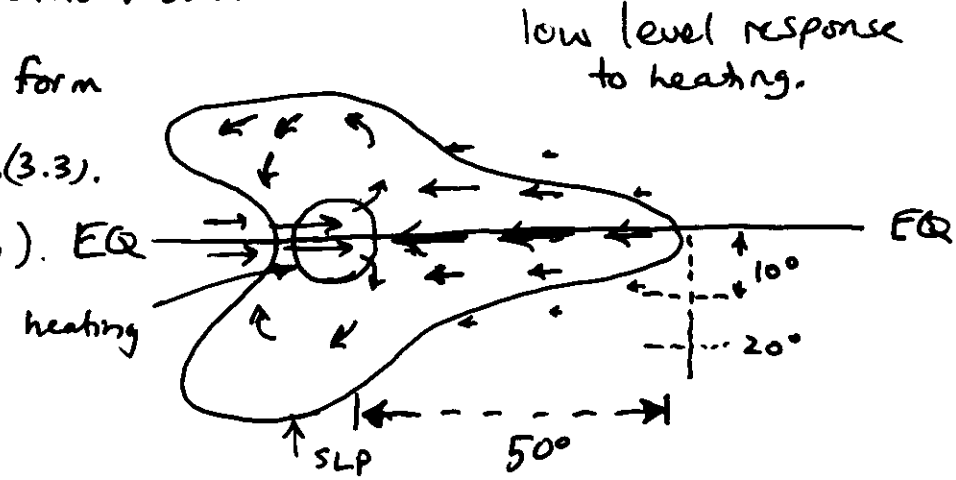

(C.) The Relationship between convective heating and SST

→ Assume local evaporation anomalies Q_{evap} will, in the steady state be balance locally by rain.

Hence, the local latent heating of the atmosphere = Q_{evap}.

- Since the surface latent heat flux is sensitive to SST changes, we have

$$Q_{evap} = Q_0 = \text{fn.of}(SST') \qquad (3.6)$$

Zebiak's (1986) "CISK" component to Gill's Model

Zebiak considered feedbacks that may result because of the anomalous circulation, driven by the local evaporation (condensation) anomalies:

The circulation initiated by Q_{evap} will drive an anomalous circulation. Hence, it will produce areas of anomalous moisture convergence

The latter will further affect the diabatic heating.

This Feedback, called CISK, is often active (in the Gill/Zebiak model) over regions where the climatological mean state is prone to convection (the ITCZ regions).

$$Q_0 = Q_{evap} + Q_{CISK}$$

- Q_0: Zebiak's heating of Gill's model
- Q_{evap}: local evaporation (funct(SST))
- Q_{CISK}: Convergence Feedback (funct.($\nabla \cdot (q\underline{v})$))

Composite Fields for Peak of ENSO warm phase

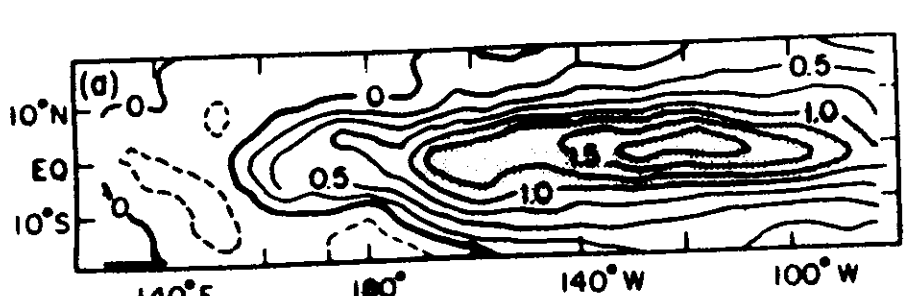

← OBSERVED SST anomalies

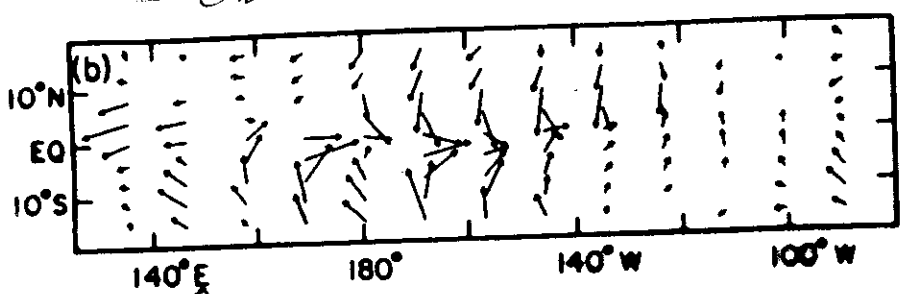

← observed wind anomalies

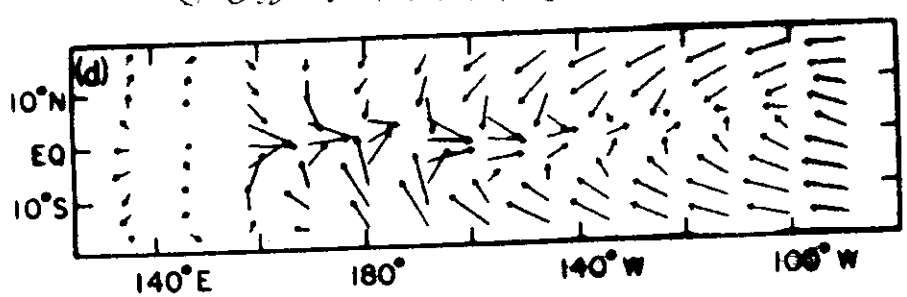

← simulated wind anomalies
(given SST in (a))

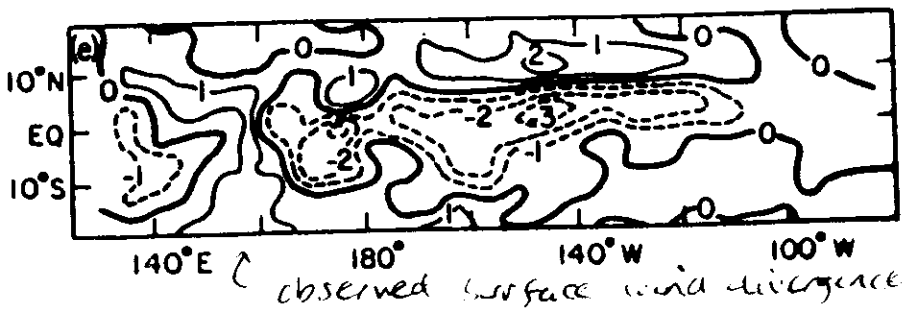

← observed surface wind divergence

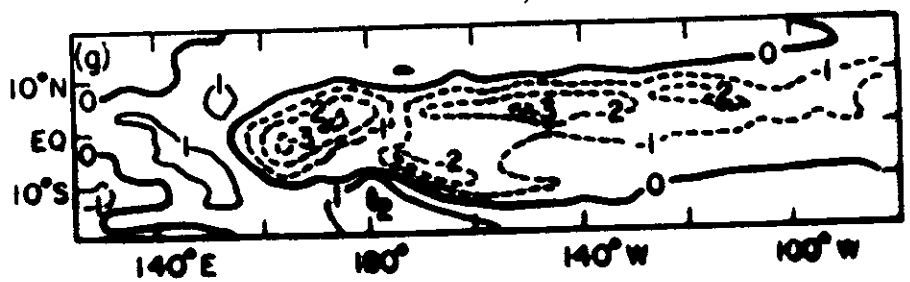

← simulated surface wind divergence

Example of Atmosphere model application (Zebiak 86)

3) THE LINDZEN/NIGAM (L/N) MODEL OF THE TROPICAL EQUILIBRIUM LOW LEVEL WIND FIELD

In the L/N model of the tropical Boundary Layer

→ Local Sea Surface Temperature anomalies drive sensible heat anomalies that change the temperature (virtual) in the boundary layer

→ Which gives rise to pressure gradients that are balanced by Coriolis torques $f\underset{\sim}{v}_{BL}$ and friction.

Fig

(a) Gill / Zebiak

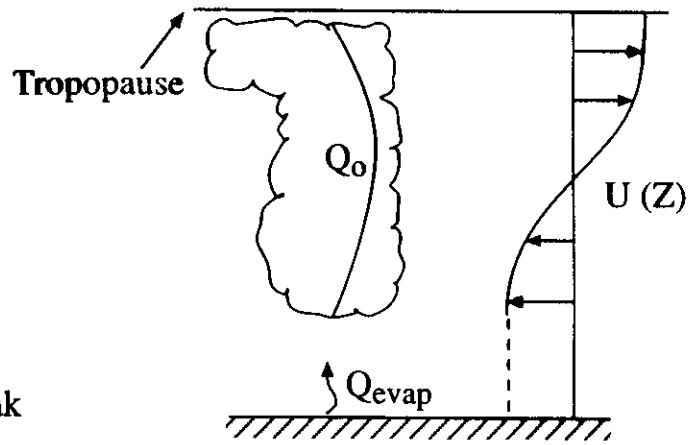

$$Q_o = Q_{evap} + Q_{conv}$$

(b) Lindzen / Nigam

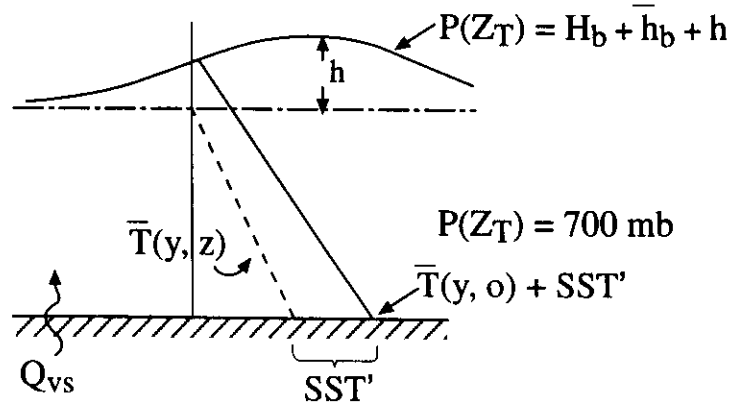

(c) Reduce Gravity

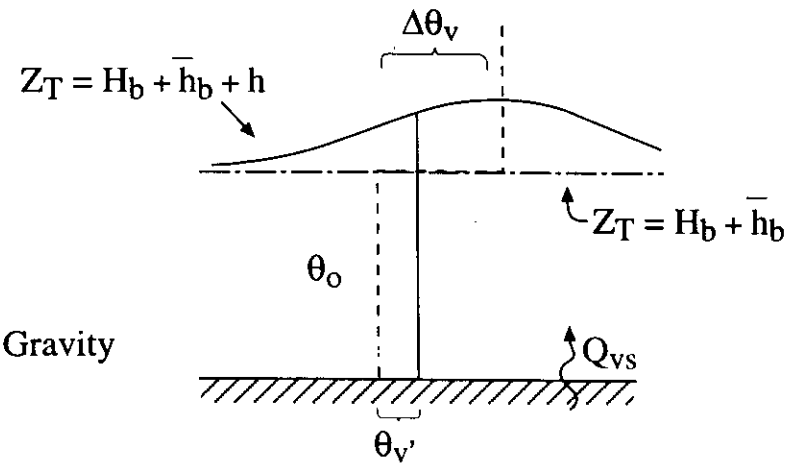

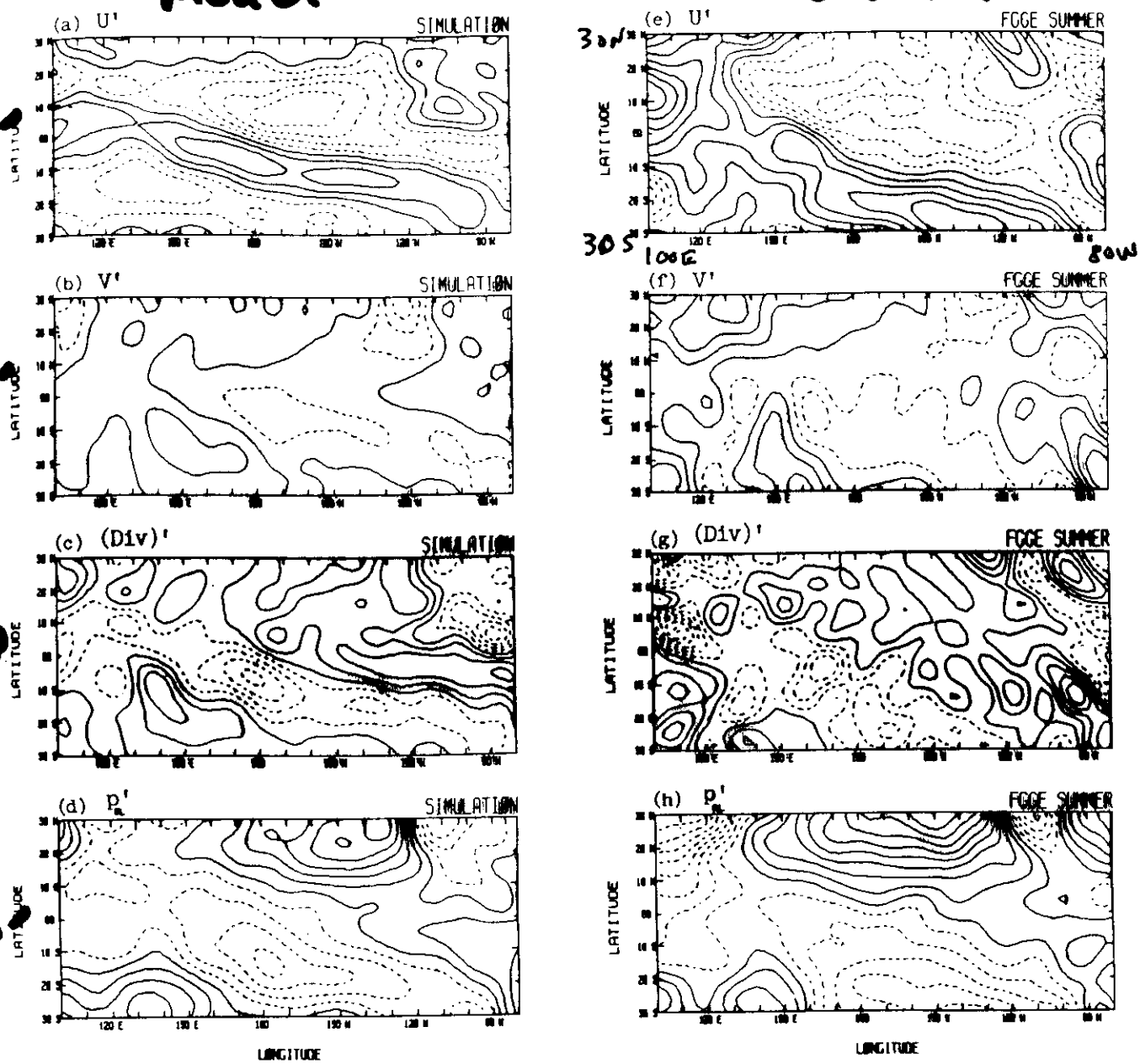

FIG. 5. The low-level summertime flow over the Pacific obtained from the linear model in which the boundary layer height is allowed to adjust to the horizontal convergence; $\epsilon = (2.5 \text{ days})^{-1}$, $\tau_c = 30$ min, $H_0 = 3000$ m. The model solutions are shown in the left panel whereas the corresponding fields from the ECMWF analysis are shown in the right panel. The contour interval is as follows: U' and $V' = 1$ m s^{-1}, div $= 4 \times 10^{-7}$ s^{-1}, and $p'_{sr} = 1$ mb; negative values are contoured using dashed lines, and the first solid contour is the zero contour.

4) THE LINDZEN/NIGAM BOUNDARY LAYER MODEL VS. THE GILL/ZEBIAK MODEL

Both deep convective heating and temperature gradients (hydrostatic PBL pressure gradients) should contribute to the solution

For coupled problem, we want surface wind stress correct (given an SST distribution)

* Which process contributes most to the surface stress?

* Which model is more relevant?

Answers: • probably the B.L. processes win over convection
• Neither model

Problems with L/N and Gill/Zebiak (Fig)

Gill/Zebiak: formally, Gill (1980) has no surface wind; (see Deser) upper troposphere nonlinear, need extraordinary damping; need 5× evaporation anomalies for given SST'.

L/N: need deep convection lifetime of 20 minutes for realistic looking solution; no inversion (PG huge).

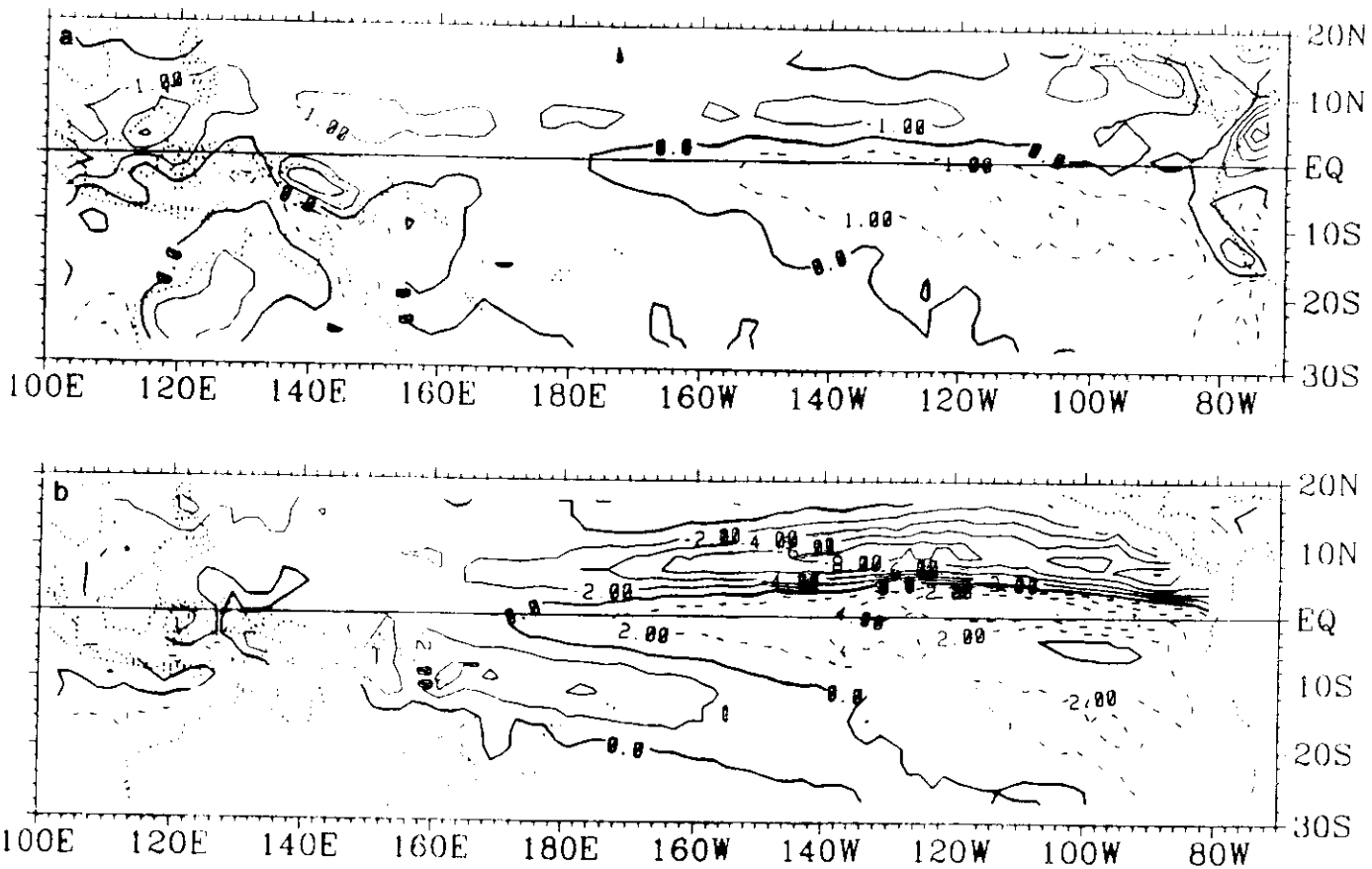

Fig. 4.4 July-November climatological mean distributions of (a) 850 mb wind divergence and (b) surface wind divergence. Units are 10^{-6} s^{-1}; negative contours are dashed. Note that the contour interval is twice as large in (b) than (a).

Minor modifications to the L/N Boundary layer model yield a model that supports realistic PBL circulations associated with prescribed "SST" forcing.

How should you view coupled models that utilize either the Gill/Zebiak or L/N models?

As using a semi-empirical atmosphere model that does a fair job at simulating the (important) observed zonal wind stress along the equator within the wave guide

5) THE EMPIRICAL ATMOSPHERE MODEL

Use the observed relationship between the surface wind (stress and heat flux) and the SST anomalies

$$\underset{\sim}{\tau}(z=0) = f_{mot}(SST);\ Q = f_{hf}(SST\ldots)$$

6) THE EXTRATROPICAL (TELECONNECTED) RESPONSE TO ANOMALOUS TROPICAL HEATING (highlights)

Tools (concepts)

- Heating produces stretching, thus vorticity production in the tropics.

$$\frac{\partial \zeta}{\partial t} + \underset{\sim}{v} \cdot \nabla (f + \zeta) \approx -f \frac{\partial \omega}{\partial p} \propto f \frac{\partial Q}{\partial p} \quad (3.7)$$

$\rightsquigarrow$ Rossby waves are generated

- The low frequency baroclinic tropospheric response is large, but remains equatorially trapped (small turning radius)

- The barotropic (deep) response has a larger turning radius

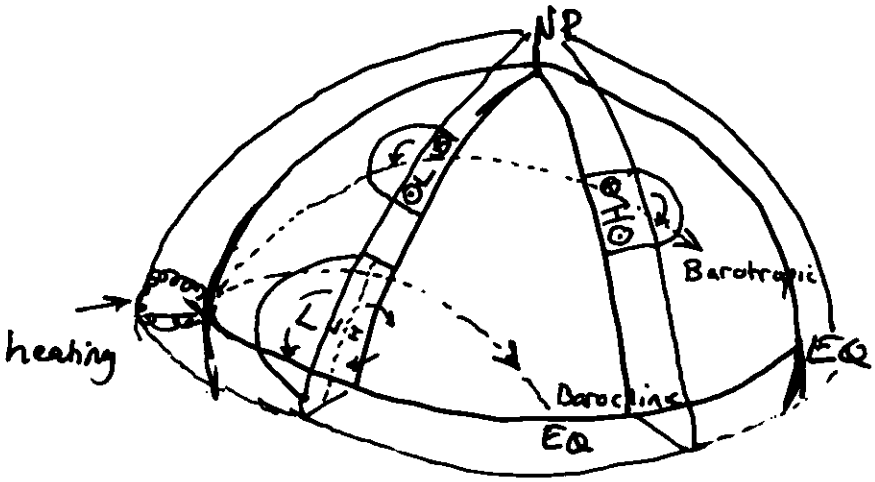

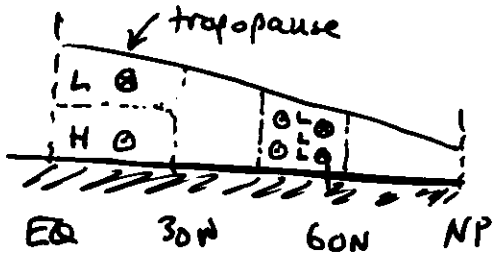

- Far field response is barotropic (mainly) poleward

- Wave path depends on shape (x, y)

Initial disturbance prototypes (both barotropic)

(a)

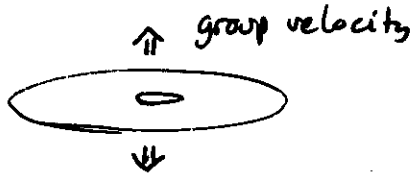

(b)

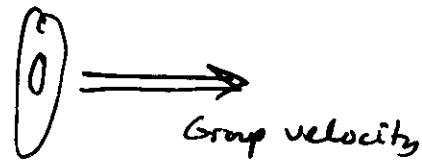

(Fig)

Hoskins
+
Karoly
1981
JAS

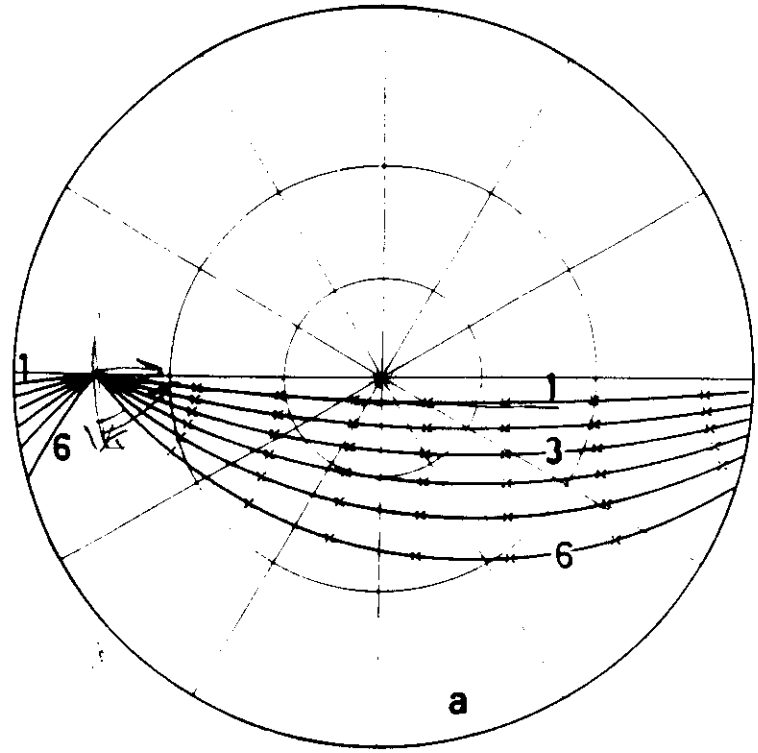

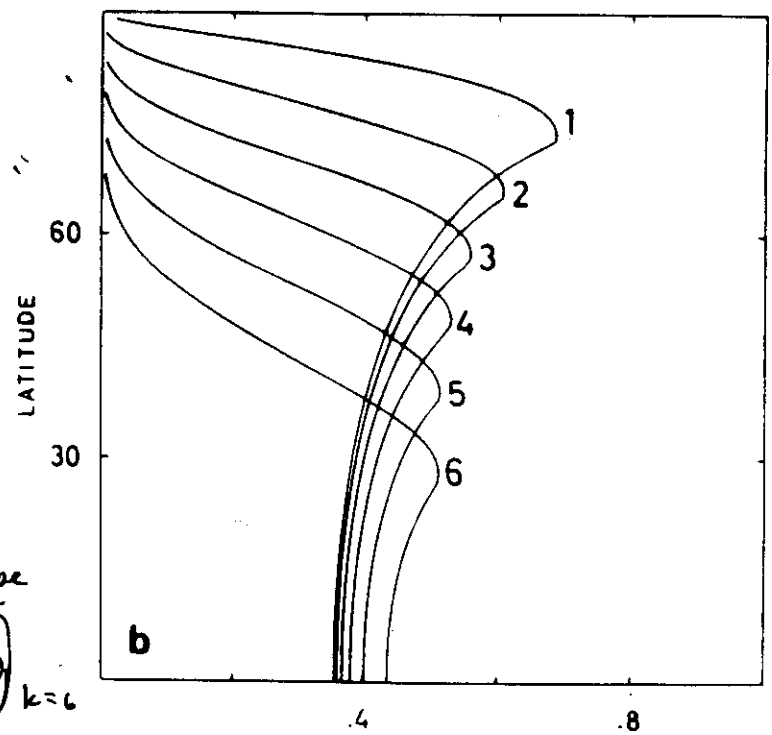

initial shape

k=1

k=6

FIG. 12. (a) Rays and phases marked by a cross every 180° for a source at 15° in a super-rotation flow. If all wavelengths give a negative extremum at the source, the crosses mark the positions of successive positive and negative extrema. Lines of latitude and longitude are drawn every 30° and the zonal wavenumbers associated with the rays are indicated. (b) Amplitudes of the extrema on the rays for the different zonal wavenumbers, on the super-rotation flow shown as a function of latitude. The relative amplitudes of the different wavenumbers depend on the position and nature of the source.

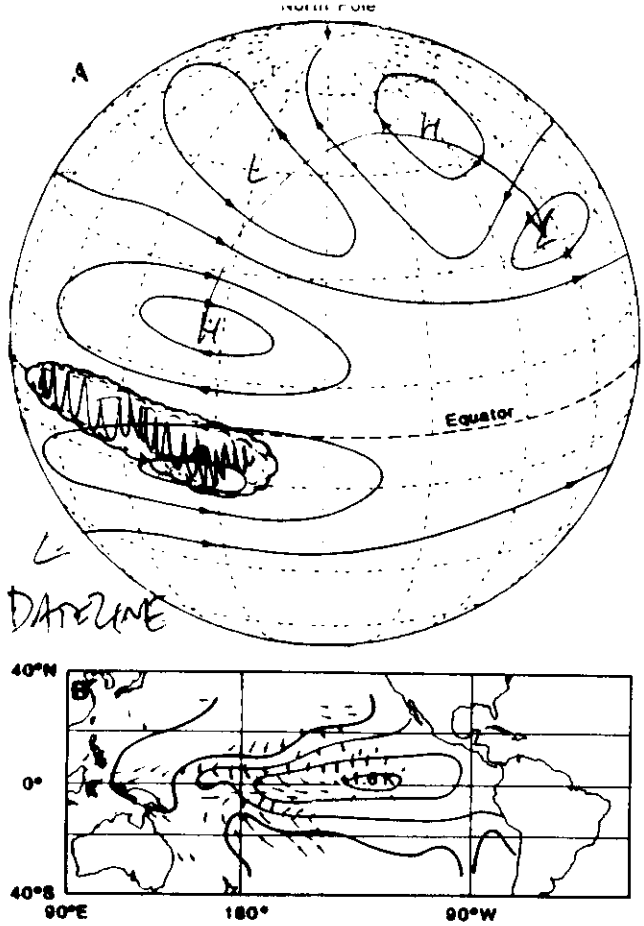

Fig. 2. Schematic illustration of atmospheric conditions during winter in the Northern Hemisphere after the peak of a typical ENSO episode, based on the understanding of the phenomenon before the 1982–1983 episode. (A) Region of enhanced precipitation (cloud outline) and circulation anomalies at the jet stream (~ 10-km) level. (B) SST and surface wind anomalies (contour interval, 0.5 K; zero contour is heavier). The longest arrows correspond to wind anomalies of ~ 1.5 m/sec (*8*, *9*).

Pacific North American Pattern (PNA) & EnSo events

Finally, the zonal deviations in the climatological mean flow (the atmospheric standing waves) affect the nature of the mid latitude teleconnected signal.

(Fig, Simmons)

- Biggest response is when the changes in the diabatic heating in the tropics are just equatorward and along the longitude of the maximum in the climatological mean jet.

because (simplistically)

the divergent meridional outflow from the heating anomaly impinges on a strong vorticity gradient

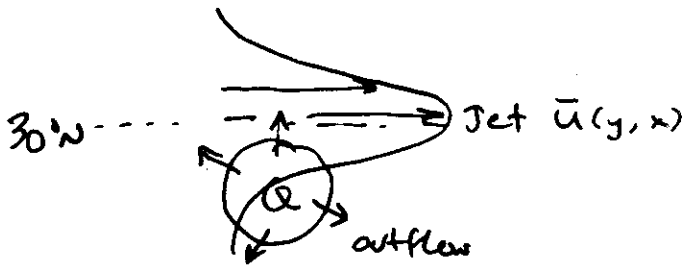

$$\frac{\partial \bar{\zeta}}{\partial t} \propto -\bar{v}' \frac{\partial \bar{\zeta}}{\partial y}$$

(Fig

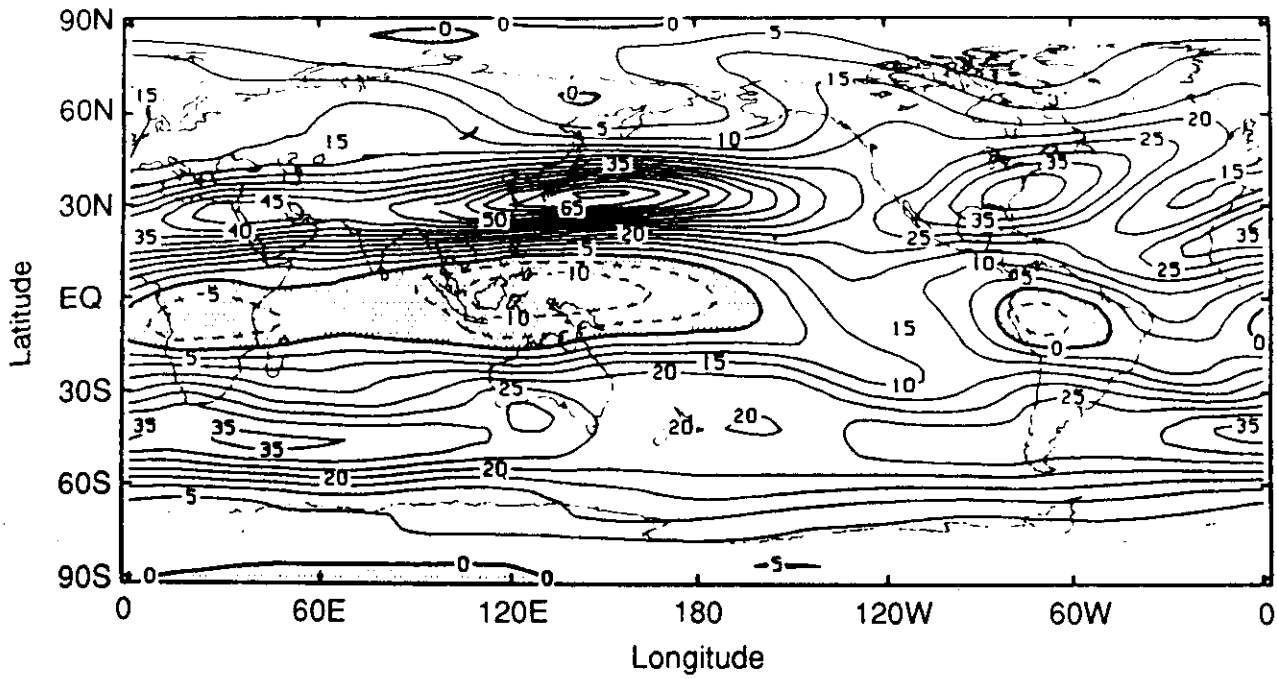

Fig. 6.2 Latitude–longitude cross section of time-averaged zonal wind speed at 200 mb for DJF averaged for years 1980–1987. (After Schubert *et al.*, 1990.)

though the equilibrium solutions shown here have not been determined in this manner but rather by direct matrix inversion as $x = -i(L - ir)^{-1}F$, it will be useful to interpret them in terms of the eigenstructure of L. Note that if any of the ω_j are close to zero, the possibility of resonance exists, and the solution becomes sensitive to the projection of F on the corresponding adjoint eigenvector $\varphi_j^{\dagger}$. The assumptions made about the dissipation r also become relatively more important in this case. In the following, we will indicate the sensitivity of our solutions to various choices of dissipation to demonstrate that our main conclusions are not affected by them.

The datasets and linear model are described in section 2. Solutions for linearization around zonally symmetric basic states are presented in section 3. The effects of introducing zonal variations in the basic states are discussed in section 4, and a summary and concluding remarks follow in section 5.

2. Datasets and linear model

The ECMWF DJF climatology used here is based upon routine daily analyses for the six winters from 1982/83 through 1987/88. The statistics are derived from a 5° × 5° lat–long version of the analyses on 12 standard pressure levels. The GCM climatology is based on a 30-year run of the GFDL GCM, made with globally prescribed boundary conditions for the years 1950 through 1979, which were available monthly and interpolated daily. The GCM's spatial discretization is rhomboidal R15 in the horizontal and nine unequally spaced levels in the vertical. More details of the ECMWF dataset can be found in Hoskins et al. (1989).

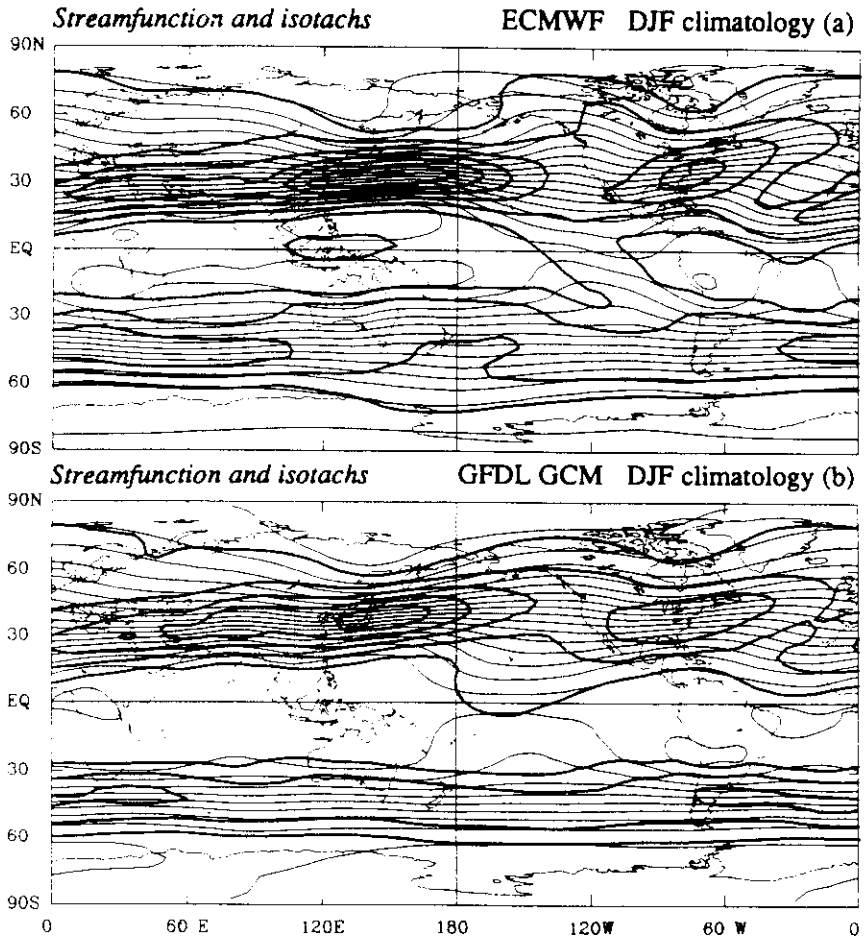

FIG. 1. DJF climatology of the horizontal wind streamfunction and isotachs (thick contours) at $\sigma = 0.205$. (a) As given by a 6-year (1982/83–1987/88) DJF average of daily initialized ECMWF analyses. (b) As given by the 30-year DJF average of a GFDL GCM run made with globally prescribed boundary conditions for the years 1950–79. Contour interval is 10^7 m^2 s^{-1} for the streamfunction and 10 m s^{-1} for the isotachs, with shading for winds stronger than 40 m s^{-1}.

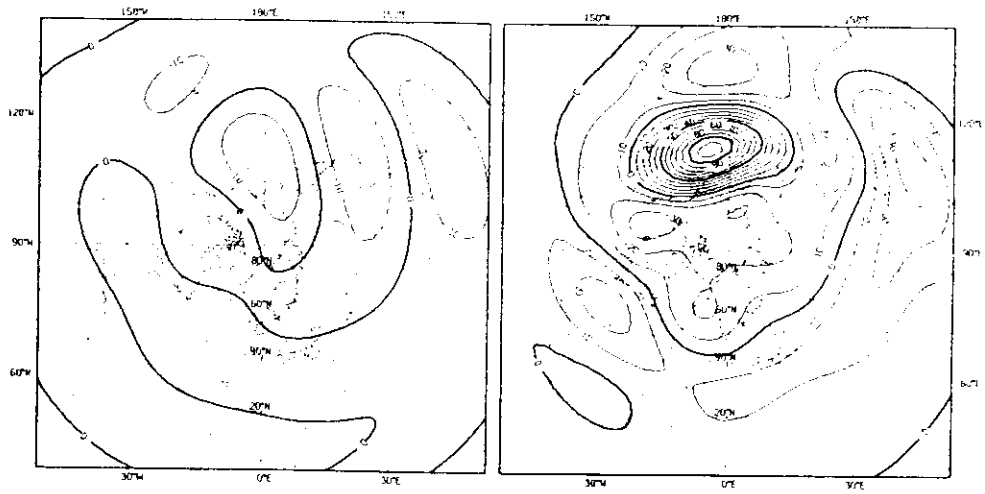

Figure 17. The response at Day 5 and Day 10 to a forcing centred at 5 °N, 135°E for a zonally-uniform climatological basic flow (left) and for the corresponding zonally-varying flow (right).

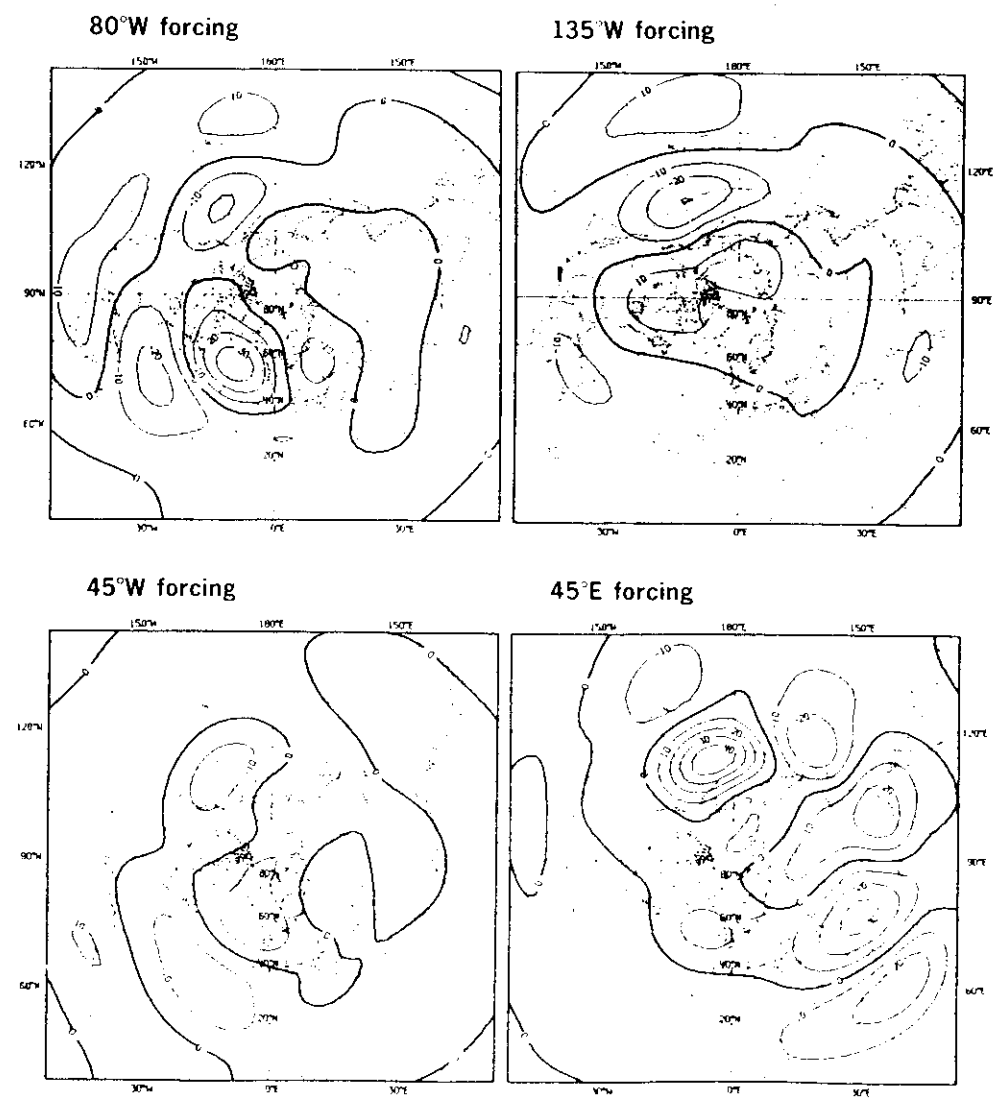

Figure 18. The response at Day 10 to forcings centred at 5 °N and various longitudes for the zonally-varying basic flow.